J|A|C|S
ARTICLES
Published on Web 06/07/2006

Topology of an Outer-Membrane Enzyme: Measuring Oxygen and Water Contacts in Solution NMR Studies of PagP

Ferenc Evanics,[†] Peter M. Hwang,[‡] Yao Cheng,[†] Lewis E. Kay,[†,‡,§] and R. Scott Prosser*,[†]

Contribution from the Departments of Chemistry, Biochemistry, and Medical Genetics and Microbiology, University of Toronto, UTM, 3359 Mississauga Road North, Mississauga, Ontario L5L 1C6, Canada

Received February 11, 2006; E-mail: sprosser@utm.utoronto.ca

Abstract: The topology of the bacterial outer-membrane enzyme, PagP, in dodecylphosphocholine micelles was studied by solution NMR using oxygen and water contacts as probes of hydrophobicity and topology. The effects of oxygen on amide protons were measured at an oxygen partial pressure of 20 atm through the paramagnetic contribution to the relaxation rates associated with the decay of two-spin order. A significant gradation of paramagnetic rates was observed for backbone amides belonging to the transmembrane residues. These rates were observed to depend on immersion depth, local hydrophobicity, and steric effects. Variations in the paramagnetic relaxation rates due to local hydrophobicity or steric effects could be, to some extent, averaged out by considering an azimuthally averaged quantity. This averaged paramagnetic rate was found to have a distinct maximum exactly in the middle of the transmembrane domain of PagP, assuming the immersion depth axis is tilted by 25° with respect to the barrel axis. Contact between the protein surface and water was assessed by measuring the amide decay rates during water saturation. The comparison of local contrast effects from both water and oxygen allows one to distinguish among steric effects, local hydrophobicity, and immersion depth. For example, the absence of contrast effects from either water or oxygen at the periplasmic end of β-strands B and C was consistent with protection effects arising from the association with the N-terminal α-helix. A parameter defined by the natural logarithm of the ratio of the normalized paramagnetic relaxation rate to the normalized amide decay rate under water saturation was found to correlate with immersion depth of the corresponding backbone amide nuclei. The results suggest that the oxygen/water contrast experiments give direct information regarding membrane protein topology and surface hydrophobicities, thereby complementing existing NMR structure studies and ESR spin-labeling studies.

Introduction

It is known that 30% of the human genome codes for membrane proteins for which we have scant structural information, while it has been estimated that 45% of all pharmaceuticals target G-protein-coupled receptors, which represent a subset of the membrane protein family.[1] There is thus a clear need for structural information about membrane protein systems. Membrane proteins also play a prominent role in genomics studies and as targets in pharmaceutical chemistry. However, structural studies of these targets by either X-ray diffraction or solution NMR are fraught with difficulty. In the case of NMR studies, significant progress has been made through the use of deuteration and pulse sequences which employ transverse relaxation optimized spectroscopic (TROSY) methods.[2−13] However, membrane proteins, in particular those consisting of transmembrane α-helical domains, often exhibit significant line broadening due to conformational exchange — a problem compounded by modest chemical shift dispersion.[9] Under such conditions, long-range nuclear Overhauser effects (NOEs) are sparse, necessitating schemes which incorporate isotopically enriched residues in otherwise perdeuterated proteins.[7] In the absence of sufficient distance information through NOEs, other structural techniques, such as those that measure orientational restraints in the form of residual dipole couplings measurements, become

[†] Department of Chemistry.
[‡] Department of Biochemistry.
[§] Department of Medical Genetics and Microbiology.

(1) Hopkins, A. L.; Groom, C. R. *Nat. Rev. Drug Discovery* **2002**, *1*, 727−730.
(2) Pervushin, K.; Riek, R.; Wider, G.; Wuthrich, K. *Proc. Natl. Acad. Sci. U.S.A.* **1997**, *94*, 12366−12371.
(3) Salzmann, M.; Pervushin, K.; Wider, G.; Senn, H.; Wuthrich, K. *Proc. Natl. Acad. Sci. U.S.A.* **1998**, *95*, 13585−13590.
(4) Fernandez, C.; Adeishvili, K.; Wuthrich, K. *Proc. Natl. Acad. Sci. U.S.A.* **2001**, *98*, 2358−2363.
(5) Hwang, P. M.; Choy, W. Y.; Lo, E. I.; Chen, L.; Forman-Kay, J. D.; Raetz, C. R. H.; Prive, G. G.; Bishop, R. E.; Kay, L. E. *Proc. Natl. Acad. Sci. U.S.A.* **2002**, *99*, 13560−13565.
(6) Hwang, P. M.; Bishop, R. E.; Kay, L. E. *Proc. Natl. Acad. Sci. U.S.A.* **2004**, *101*, 9618−9623.
(7) Tamm, L. K.; Abildgaard, F.; Arora, A.; Blad, H.; Bushweller, J. H. *FEBS Lett.* **2003**, *555*, 139−143.
(8) Fernandez, C.; Hilty, C.; Wider, G.; Guntert, P.; Wuthrich, K. *J. Mol. Biol.* **2004**, *336*, 1211−1221.
(9) Oxenoid, K.; Kirn, H. J.; Jacob, J.; Sonnichsen, F. D.; Sanders, C. R. *J. Am. Chem. Soc.* **2004**, *126*, 5048−5049.
(10) Fernandez, C.; Wuthrich, K. *FEBS Lett.* **2003**, *555*, 144−150.
(11) Roosild, T. P.; Greenwald, J.; Vega, M.; Castronovo, S.; Riek, R.; Choe, S. *Science* **2005**, *307*, 1317−1321.
(12) Tian, C. L.; Breyer, R. M.; Kim, H. J.; Karra, M. D.; Friedman, D. B.; Karpay, A.; Sanders, C. R. *J. Am. Chem. Soc.* **2005**, *127*, 8010−8011.
(13) Oxenoid, K.; Chou, J. J. *Proc. Natl. Acad. Sci. U.S.A.* **2005**, *102*, 10870−10875.

10.1021/ja0610075 CCC: $33.50

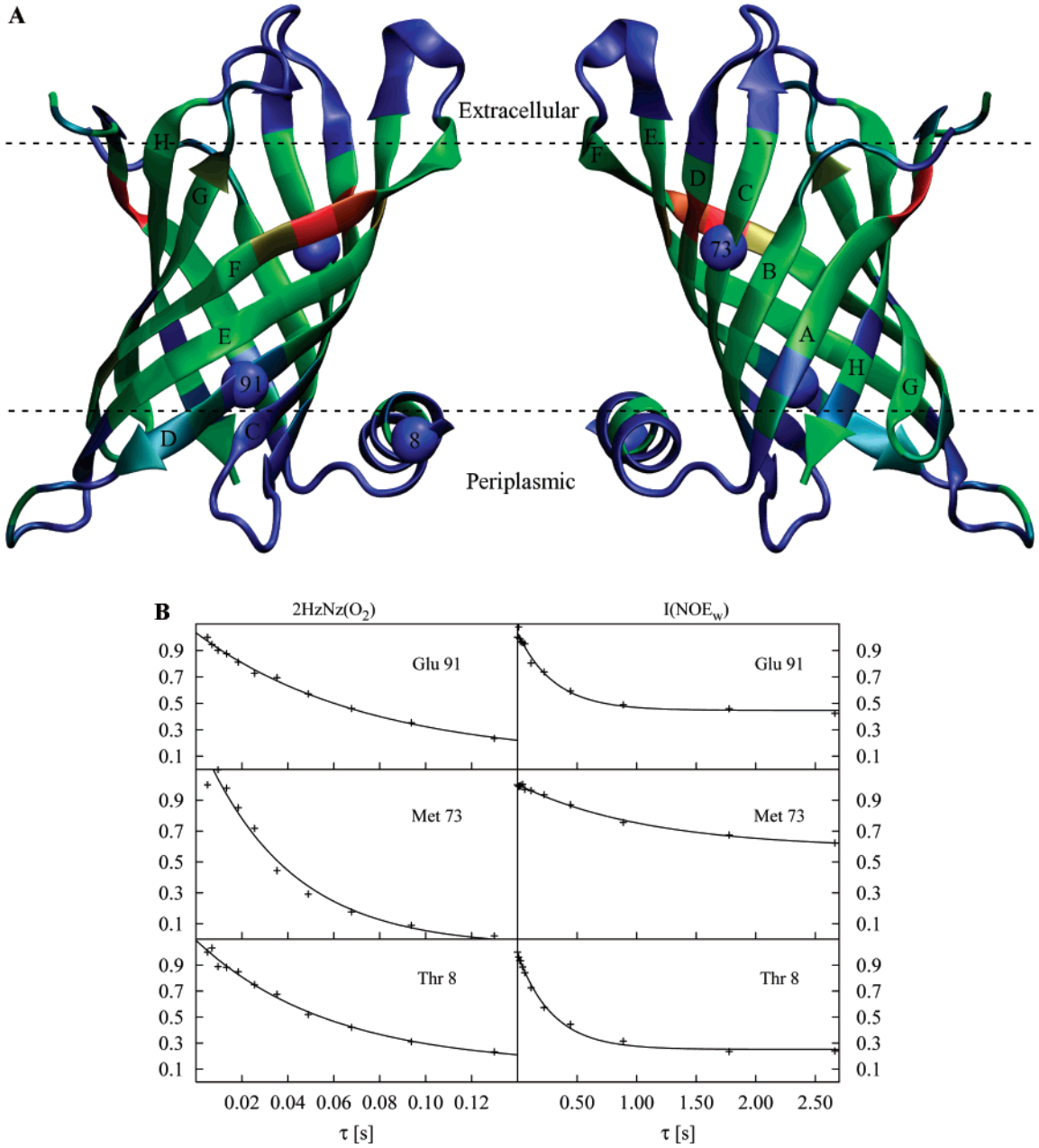

Figure 1. (A) Two perspectives of PagP, in which the barrel axis is shown tilted 25° from the membrane normal.[20] Note that the protein is colored according to local hydrophibicities (as discussed in the text), where red designates the most hydrophobic, green designates moderate hydrophobicity, and blue represents hydrophilic regions. Dashed lines represent the membrane−water interface. (B) Characteristic amide intensity decay profiles, resulting either from presaturation of water over a range of mixing times or from the preparation of longitudinal two-spin order, $2H_ZN_Z$, in the presence of oxygen, 20 atm P_{O_2}. The fastest decays of $2H_ZN_Z$ arise from residues in the most hydrophobic regions, while those residues nearest the water interface are generally those that decay most rapidly upon saturation of water.

particularly important.[13−15] NOEs to the detergent milieu define topology and establish transmembrane domains,[16−18] while local paramagnetic relaxation from nitroxide spin-labels, positioned in the micelle or in the protein via site-directed spin-labeling (SDSL),[11] all help to assemble a high-resolution structure.

In this paper, we revisit the bacterial outer-membrane enzyme, PagP, an 18 kDa protein which catalyzes palmitate transfer from a phospholipid to a glucosamine unit of lipid A.[19] The ribbon diagram, shown in Figure 1A, which is based on a 1.9 Å X-ray crystal structure,[20] features a prominent hydrophobic binding cleft on the extracellular side of the membrane, within the barrel formed by eight antiparallel β-strands. The protein barrel axis is suggested to possess a tilt of 25° with respect to the membrane normal.

(14) Ma, C.; Opella, S. J. *J. Magn. Reson.* **2000**, *146*, 381−384.
(15) Chou, J. J.; Kaufman, J. D.; Stahl, S. J.; Wingfield, P. T.; Bax, A. *J. Am. Chem. Soc.* **2002**, *124*, 2450−2451.
(16) Losonczi, J. A.; Olejniczak, E. T.; Betz, S. F.; Harlan, J. E.; Mack, J.; Fesik, S. W. *Biochemistry* **2000**, *39*, 11024−11033.
(17) Fernandez, C.; Hilty, C.; Wider, G.; Wuthrich, K. *Proc. Natl. Acad. Sci. U.S.A.* **2002**, *99*, 13533−13537.
(18) Roosild, T. P.; Greenwald, J.; Vega, M.; Castronovo, S.; Riek, R.; Choe, S. *Science* **2005**, *307*, 1317−1321.
(19) Bishop, R. E.; Gibbons, H. S.; Guina, T.; Trent, M. S.; Miller, S. I.; Raetz, C. R. H. *EMBO J.* **2000**, *19*, 5071−5080.
(20) Ahn, V. E.; Lo, E. I.; Engel, C. K.; Chen, L.; Hwang, P. M.; Kay, L. E.; Bishop, R. E.; Prive, G. G. *EMBO J.* **2004**, *23*, 2931−2941.

PagP is distinguished by two additional structural features: a β-bulge at Pro28, near the extracellular end of strand A, and an amphipathic N-terminal α-helix, α_1, which is closely associated with the periplasmic ends of strands B and C and is diagonally opposite the β-bulge. Recently, solution NMR studies have identified two interconverting states of PagP, designated as R and T, using a detergent that supports enzymatic activity.[6] Transient openings were proposed to facilitate transfer of the substrate palmitate chain to the extracellular hydrophobic binding cleft of PagP in the R-state. The protein subsequently converts to the T-state, wherein the L_1 loop and nearby regions adopt the proper conformation for catalysis. In the present study of PagP, relaxation rate measurements and water saturation experiments were confined to 45 °C and to a detergent system (dodecylphosphocholine (DPC) micelles) where the R-state dominates.

In the spirit of pioneering work by Hubbell and co-workers,[21] who made use of SDSL and contrast effects from oxygen- and water-soluble paramagnetic species, we present a solution NMR approach to the study of structure and topology of membrane proteins through the use of complementary hydrophobic and hydrophilic species, namely, oxygen and water. Effects of oxygen may be simultaneously measured on all resolvable amides by monitoring the difference in relaxation rates of two-spin order, $2H_ZN_Z$, under nitrogen from those under oxygen. Similarly, the extent of interaction with water can also be assessed by monitoring the decay of amide intensity as a function of a water presaturation time. Based on these two parameters, it becomes possible to assess local hydrophobicity, steric or protection effects, tilt of the barrel axis, and immersion depth, in a manner analogous to the ESR approach.

Oxygen is an ideal paramagnetic contrast agent for NMR studies of membrane proteins.[22−24] It can be easily added (or removed) after equilibration at an appropriate partial pressure, while it is uncharged and less perturbing than traditional contrast agents and should sample convoluted protein surfaces due to its small cross-sectional area. At modest partial pressures (20 atm oxygen), ^{1}H or ^{19}F spin−lattice relaxation times may range from 0.5 s to 50 ms in membranes. This range of rates arises from local topology[25,26] and from a pronounced oxygen solubility gradient which parallels the disorder gradients observed in membranes and micelles. The resulting transmembrane paramagnetic gradient facilitates studies of immersion depth and membrane protein topology. Moreover, because to a good approximation the NMR spin probes are relaxed by a dipolar mechanism where the only correlation times which appear in the spectral density terms are associated with the electronic spin−spin and spin−lattice relaxation times (on the order of 7 ps[27]), analysis of paramagnetic effects can be made without consideration of the dynamics of the oxygen−probe interaction.

In what follows, we show that NMR measurements of contrast effects from both oxygen and water provide a new avenue toward obtaining structural information about membrane proteins that complements the more traditional NMR approaches that are based on the measurement of distances. An application of the methodology to PagP provides (i) insight into the position of the N-terminal helix relative to the β-barrel of the enzyme, (ii) evidence of tilt of the barrel axis, and (iii) information about the overall topology of the protein in the R-state, when incorporated into micelles. Much of the data obtained is not accessible by other NMR approaches.

Materials and Methods

Sample Preparation and NMR Experiments. ^{2}H,^{15}N-labeled PagP was expressed from *Escherichia coli* and incorporated into perdeuterated DPC (Cambridge Isotopes, Andover, MA) micelles as described previously,[5] with final protein and detergent concentrations of 1.0 and 200 mM, respectively. A TROSY version of an $2H_ZN_Z$ relaxation experiment[28−30] was performed at 45 °C, under a partial pressure of 20 atm (oxygen or nitrogen), using a Varian Inova 600 MHz spectrometer and sapphire NMR tubes (Saphikon, NH) with a 5 mm o.d. and 3 mm i.d. The paramagnetic component of the decay rates associated with two-spin order was determined by measuring the difference in decay rates under nitrogen from those under oxygen. Typically, 64 scans and 80 increments were acquired for each ^{1}H−^{15}N TROSY spectrum, while 7 relaxation delays ranging from 4 to 130 ms (O_2) or from 20 to 220 ms (N_2) were used with a repetition time of 1 s (O_2) or 2.4 s (N_2). Typical decay profiles associated with longitudinal two-spin order (under oxygen) are shown for several residues in Figure 1B. Note, for example, that the amide group associated with Met 73, which resides in the hydrophobic interior, exhibits a rapid decay of two-spin order in the presence of oxygen. All experiments were performed in 10% D_2O to obtain a reliable lock signal.

Water NOE measurements were performed using low-power water saturation pulses (i.e., a 30 Hz B_1 field) ranging in time from 50 ms to 2.2 s, with a total of 11 mixing times. To minimize relayed effects from water saturation while striving to obtain a large dynamic range of contrast effects from water, the protein under study was 85% deuterated, as a result of expressing PagP in deuterated water, while perdeuterated detergents were also used exclusively. Water exchange rates in the fully accessible loop regions were also obtained via a TROSY version of the CLEANEX-PM clean chemical exchange spectroscopy sequence. NOE intensities to water[31,32] showed that the residence times of many of the water molecules were at least on the order of several nanoseconds, with the exception of those of molecules that interact with residues that are exposed.

Results and Discussion

Transmembrane Regions and Local Hydrophobicity Effects by NMR/O_2 Experiments. In the lipid bilayer or micelle hydrophobic interior, oxygen solubility ranges between 3 and 10 times that of water.[33,34] Therefore, contrast effects of oxygen are expected to be highest for residues directly associated with the micelle interior or possibly with the hydrophobic binding

(21) Altenbach, C.; Marti, T.; Khorana, H. G.; Hubbell, W. L. *Science* **1990**, *248*, 1088−1092.
(22) Prosser, R. S.; Luchette, P. A.; Westerman, P. W. *Proc. Natl. Acad. Sci. U.S.A.* **2000**, *97*, 9967−9971.
(23) Prosser, R. S.; Luchette, P. A.; Westerman, P. W.; Rozek, A.; Hancock, R. E. W. *Biophys. J.* **2001**, *80*, 1406−1416.
(24) Luchette, P. A.; Prosser, R. S.; Sanders, C. R. *J. Am. Chem. Soc.* **2002**, *124*, 1778−1781.
(25) Teng, C. L.; Bryant, R. G. *J. Am. Chem. Soc.* **2000**, *122*, 2667−2668.
(26) Hernandez, G.; Teng, C. L.; Bryant, R. G.; LeMaster, D. M. *J. Am. Chem. Soc.* **2002**, *124*, 4463−4472.
(27) Teng, C. L.; Hong, H.; Kiihne, S.; Bryant, R. G. *J. Magn. Reson.* **2001**, *148*, 31−34.
(28) Salzmann, M.; Wider, G.; Pervushin, K.; Wuthrich, K. *J. Biomol. NMR* **1999**, *15*, 181−184.
(29) Pervushin, K.; Riek, R.; Wider, G.; Wüthrich, K. *Proc. Natl. Acad. Sci. U.S.A.* **1997**, *94*, 12366−12371.
(30) Yang, D. W.; Kay, L. E. *J. Biomol. NMR* **1999**, *13*, 3−10.
(31) Gemmecker, G.; Jahnke, W.; Kessler, H. *J. Am. Chem. Soc.* **1993**, *115*, 11620−11621.
(32) Hwang, T. L.; Mori, S.; Shaka, A. J.; vanZijl, P. C. M. *J. Am. Chem. Soc.* **1997**, *119*, 6203−6204.
(33) Nielsen, R. D.; Che, K. P.; Gelb, M. H.; Robinson, B. H. *J. Am. Chem. Soc.* **2002**, *127*, 6430−6442.
(34) Al-Abdul-Wahid; Yu, C. H.; Batruch, I.; Evanics, F.; Pomès, R.; Prosser, R. S. *Biochemistry* **2006**, submitted.

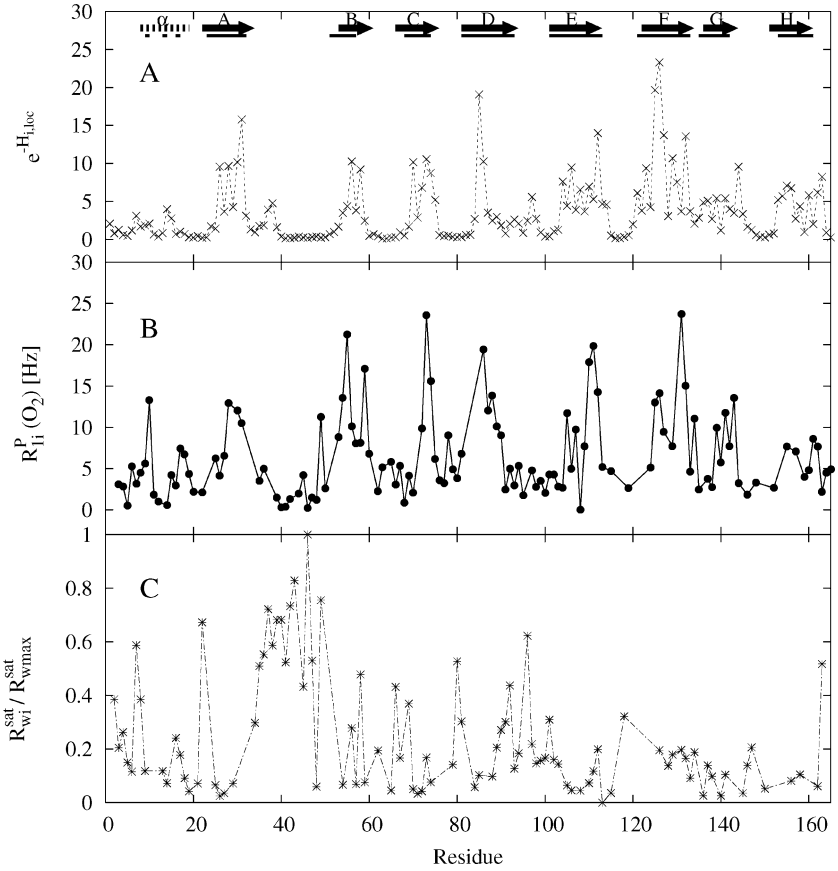

Figure 2. (A) Estimation of the Boltzmann factor associated with local protein hydrophobicity [i.e., $\exp(-H_{i,\mathrm{loc}}/RT)$] as a function of residue. The locally averaged hydrophobicity, $H_{i,\mathrm{loc}}$, is determined by a weighted average involving the hydrophobicity of the source residue, the average hydrophobicity of all residues within 3 Å, and the average hydrophobicity of residues within a shell between 3 and 6 Å away from the source residue. (B) Paramagnetic relaxation rate, $R^{\mathrm{p}}_{1i}(\mathrm{O}_2)$, versus residue. (C) Decay rate arising from water saturation, R^{sat}_{wi}, as a function of residue.

pocket of the PagP enzyme. The transmembrane regions are thus identified by characteristically higher paramagnetic rates, $R^{\mathrm{p}}_{1i}(\mathrm{O}_2)$, as shown in Figure 1B, where typical decay curves of longitudinal two-spin order in the presence of oxygen are dramatically steeper, for residues such as Met-73, in the transmembrane region than those from extracellular or periplasmic domains. Note that relatively high accessibility to oxygen, which is indicative of a hydrophobic region, is most often correlated with a relatively low degree of water contact, as shown by the amide intensity profiles as a function of water saturation times in Figure 1B.

The overall $R^{\mathrm{p}}_{1i}(\mathrm{O}_2)$ profile is shown in Figure 2B, where the regions in which $R^{\mathrm{p}}_{1i}(\mathrm{O}_2)$ is highest correspond to residues associated with the transmembrane β-strands. ESR and NMR studies which have made use of contrast effects of oxygen acting on site-directed spin-labels or site-directed ^{19}F labels report a significant gradient of effects with immersion depth.[22−24] Previous studies have found that the oxygen solubility profile, and thus the paramagnetic contrast effect, is approximately Gaussian[35] or Boltzmann-sigmoidal.[36] In either case, the contrast effect is expected to increase monotonically with immersion depth, assuming neither steric effects nor local protein surface hydrophobicity is significant. However, there is a distinction to be made in this study since the backbone amide label does not necessarily extend into the detergent milieu as would a side-chain label. Therefore, we expect the oxygen solubility and corresponding contrast effect on a given residue to depend, at least in part, on local hydrophobicity of the protein, $H_{i,\mathrm{local}}$. To investigate this, we consider the hydrophobicity of a given residue, H_i, according to the Kyte−Doolittle scale.[37] We define the local hydrophobicity, $H_{i,\mathrm{local}}$, by averaging the hydrophobicity of the *i*th residue, H_i, with the average hydrophobicity of all residues within 3 Å of the source, $\langle H_i^{<3\text{Å}}\rangle$, plus the average hydrophobicity of those residues in a shell between 3 and 6 Å from the source, $\langle H_i^{3-6\text{Å}}\rangle$, such that

$$H_{i,\mathrm{local}} = \frac{1}{3}H_i + \frac{1}{3}\langle H_i^{<3\text{Å}}\rangle + \frac{1}{3}\langle H_i^{3-6\text{Å}}\rangle \qquad (1)$$

Here, the X-ray crystal structure[19] is used to determine those residues within a 3−6 Å radius of the residue in question. The overall free energy associated with local oxygen solubility is expected to include an immersion-depth-dependent term associated with the micelle surroundings in addition to the above term associated with the local hydrophobicity, and the solubility would be proportional to the exponential of the free energy. If we revisit the $R^{\mathrm{p}}_{1i}(\mathrm{O}_2)$ relaxation profile in Figure 2B, we notice that, although there are rate enhancements in the transmembrane domain, there are several points where the paramagnetic rate associated with a particular residue seems

(35) Windrem, D. A.; Plachy, W. Z. *Biochim. Biophys. Acta* **1980**, *600*, 655−665.
(36) Dzikovski, B. G.; Livshits, V. A.; Marsh, D. *Biophys. J.* **2003**, *85*, 1005−1012.
(37) Kyte, J.; Doolittle, R. F. *J. Mol. Biol.* **1982**, *157*, 105−132.

anomalously low relative to its immersion depth. For example, a dip in $R_{1i}^{P}(O_2)$ can be found near the middle of most transmembrane strands. Moreover, these variations are completely reproducible; fitting errors are on the order of 5−10%, but a very similar paramagnetic rate profile was also obtained by measuring the change of spin−lattice relaxation rates upon oxygenation (data not shown). Furthermore, the maxima associated with certain transmembrane strands (particularly G and H) are also reproducibly lower than those in other strands. This can be explained, in part, by examining the exponential of the above local hydrophobicity as a function of residue, shown by the dashed line in Figure 2A. Even without considering any steric factors or immersion depth effects, it appears that there is some correlation between the oxygen contrast effect and the local protein hydrophobicity. Thus, we conclude that the essential features of the paramagnetic rate data arise from the immersion-depth-dependent concentration gradient of oxygen in the surrounding detergent milieu. However, the distinct rate variations seen for residues associated with a given transmembrane strand can be attributed, in part, to local variations of protein hydrophobicity. In situations where the probe is attached to the terminus of a side chain, as in SDSL studies[21,28] or studies of methyl groups,[38−40] it is expected that the hydrophobicity and consequent contrast effects with water and oxygen would be governed in a more pronounced manner by the surrounding environment rather than by local protein hydrophobicities.

Transmembrane Regions and Orientation of the Barrel Axis by NMR/O_2 Experiments. As a result of the recent X-ray crystallography study of PagP cocrystallized in lauryl dimethylamine oxide, the authors postulated that the β-barrel axis was tilted by 25° with respect to the membrane normal, since this orientation clusters the aromatic side chains near the membrane−water interface − a feature common to many membrane proteins.[41] Under these circumstances, the number of residues required to span the membrane will range from 6−8 residues (strands A, B, and H) to as many as 12 residues (strands D, E, and F, which are tilted by roughly 50° relative to the membrane normal).[20] In principle, the number of transmembrane residues per strand should be straightforward to measure from the paramagnetic rate profiles, since residues spanning the micelle interior exhibit distinctly higher relaxation rates. However, due to missing residue information and the influence of local steric effects, it is difficult to assess the tilt in this way.

An alternative means of considering the issue of tilt of the barrel axis of PagP is to examine the average paramagnetic rate profile as a function of immersion depth. Here, we assume the immersion depth axis is either along the PagP barrel axis or tilted by 25°, as shown in Figure 3A. In either model, the detergent coating resembles the outer surface of a torroid. Note that the detergents are proposed to minimally coat the hydrophobic belt of transmembrane residues from PagP, in such a way as to adopt a radius of curvature that minimizes the micelle free energy. The long-standing image of the arrangement of amphiphiles such as micellar detergents or bilayer lipids, as proposed originally by Dill and Flory,[42] is one in which a distinct disorder gradient exists along the immersion depth axis (i.e., perpendicular to the micelle surface). As such, we expect the azimuthally averaged paramagnetic rate to reflect the oxygen concentration profile, which is known to increase monotonically toward the location of greatest disorder or, equivalently, greatest immersion depth (i.e., $z = 0$, designated by the dashed horizontal line in Figure 3A) in both micelles and lipid bilayers.[21,33]

To assess the azimuthally averaged depth-dependent rates, the X-ray crystal structure of PagP was oriented in one of two ways, as proposed in Figure 3A. The system was next divided into a series of 2-Å-thick slices along the immersion depth axis. All resolvable amides whose positions were within a given slice, $z \pm 1$ Å, were used to determine the average rate. An azimuthally averaged rate should be less susceptible to local variations in paramagnetic rates due to either steric effects or anomalous local hydrophobicities. Figure 3B reveals the experimentally determined average paramagnetic rate, $R_1^P(z)$, as a function of immersion depth for both the tilted and untilted barrel models. The resultant trace in Figure 3B is a reasonably symmetric function whose maximum lies exactly at the membrane center ($z = 0$) for the model in which PagP is proposed to be tilted by 25°, in contrast to the result for the untilted model, where the maximum lies 6 Å farther away. Since oxygen solubilities (and thus contrast effects) are known to be greatest in the membrane or micelle interior (i.e., $z = 0$),[34,43] we conclude that the barrel axis adopts a tilted conformation in micelles in solution, consistent with expectations based on the crystal structure.[20]

Similar depth-dependent contrast effects have been observed previously with membrane proteins solubilized in detergents[43−46] using water-soluble paramagnetic species or detergents in which a spin-label is attached to a given carbon on the chain. Interestingly, such effects have been measured on a membrane-associated protein, α-synuclein, in sodium dodecyl sulfate micelles in ESR[43] and NMR[47] studies of the relaxation of both backbone and side-chain nuclei. In the case of the NMR work, the same depth-dependent contrast effects that were obtained via ESR could be observed upon the addition of detergents bearing spin-labels at specific carbons on the chain. However, backbone nuclei were noted to give local variations which were attributed to the protection factor associated with the side chain. Such subtleties and fine structure associated with contrast effects acting on the backbone nuclei are not unexpected and are observed in our experiments using oxygen or water (vide infra) as contrast agents. In any case, the agreement between ESR and NMR experiments on the topology of α-synuclein reinforces the idea that immersion depth and, indeed, topological data can, in principle, be obtained on membrane proteins in micelles.

Using Water To Complement NMR/O_2 Measurements. Though oxygen is clearly a useful paramagnetic probe of topology, as evidenced by the above results, we consider next whether additional measurements of contact with water might

(38) Tugarinov, V.; Kay, L. E. *Chembiochem* **2005**, *6*, 1567−1577.
(39) Kay, L. E. *J. Magn. Reson.* **2005**, *173*, 193−207.
(40) Tugarinov, V.; Hwang, P. M.; Ollerenshaw, J. E.; Kay, L. E. *J. Am. Chem. Soc.* **2003**, *125*, 10420−10428.
(41) de Planque, M. R. R.; Killian, J. A. *Mol. Membr. Biol.* **2003**, *20*, 271−284.
(42) Dill, K. A.; Flory, P. J. *Proc. Natl. Acad. Sci. U.S.A.* **1981**, *78*, 676−680.
(43) Bussell, R., Jr.; Ramlall, T. F.; Eliezer, D. *Protein Sci.* **2005**, *14*, 862−872.
(44) Brown, L. R.; Braun, W.; Kumar, A.; Wuthrich, K. *Biophys. J.* **1982**, *37*, 319−328.
(45) Papavoine, C. H. M.; Konings, R. N. H.; Hilbers, C. W.; van de Ven, F. J. M. *Biochemistry* **1994**, *33*, 12990−12997.
(46) Brunecky, R.; Lee, S.; Rzepecki, P. W.; Overduin, M.; Prestwich, G. D.; Kutateladze, A. G.; Kutateladze, T. G. *Biochemistry* **2005**, *44*, 16064−16071.
(47) Bisaglia, M.; Tessari, I.; Pinato, L.; Bellanda, M.; Giraudo, S.; Fasano, M.; Bergantino, E.; Bubacco, L.; Mammi, S. *Biochemistry* **2005**, *44*, 329−339.

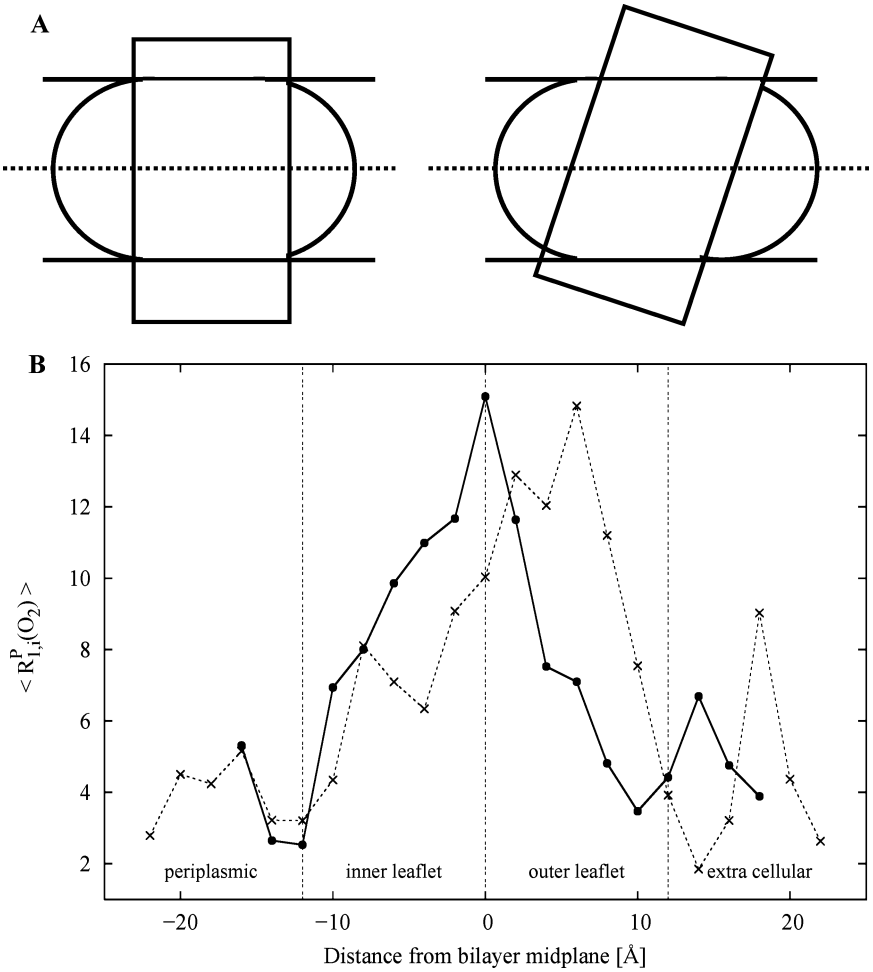

Figure 3. (A) Two models of the tilt of PagP in an idealized version of a micelle. In the first case, the immersion depth axis is proposed to be along the barrel axis, while in the latter case, the immersion depth axis is tilted by 25°. Note that the oxygen solubility profile should parallel the disorder profile of the micelle, reaching a maximum at the position indicated by the dashed line. (B) Average paramagnetic rates, $R^{P}_{1i}(O_2)$, as a function of immersion depth, *z*. To determine an average rate, the system was divided into 2-Å slices, whereupon $R^{P}_{1i}(O_2)$ rates were averaged within a given slice. Two distinct profiles are obtained, depending on whether the immersion depth axis is chosen to be tilted by 25° from the barrel axis, as proposed by Ahn et al.[20] (solid line), or along the barrel axis (dashed line).

complement the oxygen contrast experiments. To assess water contact, we have measured the effect of water presaturation on amide proton intensity in an ^{15}NH TROSY experiment. In principle, the decay of amide intensity, I_i, with water saturation time, τ_{sat}, should depend on a number of factors, including the selective T_1 relaxation time of the amide proton, water chemical exchange, dipolar exchange mechanisms, and residual relayed spin effects. With the possible exception of spin−lattice relaxation, amide decay arising from chemical or dipolar exchange is expected to be sensitive to the extent of water accessibility. All effects together can provide a measure of contact with water. In our experiments, most decays were found to fit well to a single-exponential decay of the form, $I_i = A \exp(-R^{sat}_{wi}\,\tau_{sat}) + B$, where A and B are simple fitting constants and R^{sat}_{wi} specifies the resulting amide decay rate. Here our interest lies simply in qualitatively estimating the degree of contact with water, operating under the assumption that a distinct gradient of water solubility exists along the micelle immersion depth axis.[35] In the presence of such gradients, amide decay rates from water saturation are expected to decrease with immersion depth. Equilibrium intensities [i.e., $B/(B + A)$] resulting from water saturation for 2−3 s were also obtained and were found to range from 0.02 to 0.98 times the initial intensity. Typical amide decay profiles resulting from water presaturation are shown for several residues in Figure 1B, to convey the range of contrast effects. Note, for example, that the amide proton associated with residue Glu 91 is accessible to water and, as such, exhibits a relatively fast decay rate upon saturation of water, while the decay of two-spin order in the presence of oxygen, a hydrophobic contrast agent, is relatively slow. Conversely, Met 73, which resides in the hydrophobic interior, exhibits the opposite tendency, as seen in the rapid rate of decay of two-spin order in the presence of oxygen and slow amide decay rates associated with water presaturation. The amide proton associated with Thr 8, which is also accessible to water, exhibits modest decay rates due to oxygen and rapid decay rates upon water saturation, such that its steady-state intensity reaches less than 30% of its intensity in the absence of water presaturation. Such decay rates and steady-state levels depend on both amide spin−lattice relaxation times and accessibility to water or nearby exchanging protons. Similar profiles of R^{sat}_{wi} vs residue are obtained whether selected T_1's are or are not subtracted, and in what follows we have not removed these contributions.

Figure 2C reveals the amide decay rate profile resulting from water saturation, while Figure 4 maps these rates on the protein surface. Typically, very large contrast effects of water are

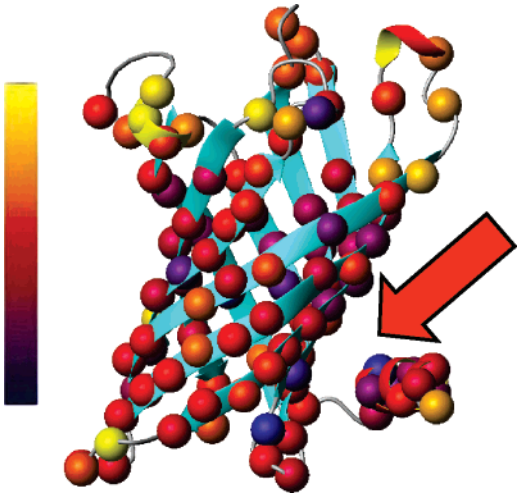

Figure 4. Three-dimensional perspective of PagP, based on amide decay rates from water saturation. Decay rates range from yellow (highest contact with water) to dark blue (lowest contact with water), as indicated by the vertical color bar. The strongest NOEs occur in the aqueous domains, while weaker decay rates are observed in the membranous regions. The arrow indicates a region in which water accessibility is observed to be low, presumably due to close interaction between the N-terminal helix and the β-barrel.

observed in the extracellular loop regions, although R_{wi}^{sat} is also significant at the N-terminus of the protein and in the first few residues of the N-terminal α-helix. The extent of water interactions with the transmembrane residues is more striking. The interfacial hydrophobic residues, associated with the aromatic belt of the protein, exhibit moderate water interactions, while most residues in the majority of transmembrane strands exhibit reduced contact with water. Note, in particular, that residues in the proposed interface between strands B and C of the β-barrel and the N-terminal helix appear darker than those at an equivalent immersion depth on the opposite side of the protein. This would be consistent with the notion that the N-terminal helix associates with the barrel, thereby reducing the extent of contact with water.

Combining Water and Oxygen Contact Information To Investigate Immersion Depth. ESR studies of spin-labeled membrane proteins have demonstrated that the ratio of line broadening or power saturation effects from a hydrophobic and hydrophilic contrast agent, such as oxygen and nickel ethylenediamine-*N*,*N*′-diacetic acid (NiEDDA), will provide a measure of immersion depth.[48] Assuming that the mobilities and sizes of the two contrast agents are similar, the ratio will be independent of steric effects and should ideally depend on the relative partitioning properties of oxygen and NiEDDA in a membrane/water system. Moreover, the natural logarithm of this ratio was shown to depend only on the difference in chemical potentials of the contrast agents, which can be approximated to depend linearly on immersion depth. Fortunately, contact with water, rather than NiEDDA, can be measured (at least qualitatively) directly by NMR. Moreover, the membrane partitioning properties of water are higher than those of NiEDDA, while the size and mobility of water are similar to those of oxygen. It has also been noted that the concentration gradients of water and oxygen are roughly opposite in membranes.[36] Therefore, it may be possible to measure the degree of contact to both oxygen and water for a given residue and, in so doing, determine the immersion depth by NMR.

In keeping with the approach taken by Altenbach et al.,[48] we define a parameter Φ_i which incorporates a ratio of the measure of contact with oxygen and water, and we consider the extent to which it correlates with immersion depth. Φ_i is defined as

$$\Phi_i \equiv \ln\{[R_{1i}^{P}(O_2)/R_{1max}^{P}(O_2)]/[R_{wi}^{sat}/R_{wmax}^{sat}]\} \qquad (2)$$

where both the oxygen and water contact terms have been normalized by dividing each by the respective maxima observed for the transmembrane residues. Figure 5 shows the dependence of the experimentally determined Φ_i with immersion depth, calculated using the 25° tilted structure of PagP (Figure 3A). Note that a linear dependence is observed, with a Pearson *r* correlation of 0.69. Though reasonable, some of the variation from linearity may arise from inadequacies of the water presaturation experiments. In particular, relayed effects will be present for an 85% deuterated protein, and it would be preferable to use fully deuterated media to reduce such artifacts. A second source of variation of the depth parameter may arise from the fact that the probe is a backbone amide residue and thus does not extend into the membrane-like milieu as would a side-chain label such as that used for ESR purposes. Although this gives us the advantage of being able to examine contrast effects of nearly every residue at once, the result is expected to be complicated by local variations of protein surface hydrophobicities. However, in situations where the probe of interest is a terminal methyl side-chain label, it is expected that the immersion depth, which arises from the surrounding membrane-like environment, could be more reliably measured.

Combining Water and Oxygen Contact Information To Investigate Steric Effects. We next consider if other combinations of the paramagnetic oxygen rates and amide decay rates under water saturation can be used to assess topological features of the protein. For example, as discussed above, the lack of significant water contact to residues from the N-terminal helix and strands B and C of the barrel (shown in Figure 4) supports the notion that the N-terminal helix associates with this region of PagP. This same argument should apply to oxygen paramagnetic rates, and the product of the two contrast effects may be more sensitive to steric factors. The recent X-ray crystal structure of PagP revealed the N-terminal α-helix to be adjacent to strands B and C, on the periplasmic side of the membrane, lying at the membrane−water interface.[20] In contrast, prior solution NMR studies in detergent micelles could not identify a distinct conformation of the helix with respect to the barrel. The NMR O_2/H_2O contrast experiments described above can, in principle, address the issue of the location of the N-terminal α-helix in detergent micelles, relative to the barrel, by identifying surface regions of the barrel and the helix which exhibit reduced contact with oxygen and water. We define a parameter for monitoring reduced contact with water and oxygen as

$$\Psi_i \equiv R_{1i}^{P}(O_2)\, R_{wi}^{sat} \qquad (3)$$

Figure 6 shows the above parameter as a function of residue for PagP. Note that several residues belonging to strands A, B, and C, on the periplasmic side near the membrane−water interface, exhibit very low Ψ_i values, suggesting that they are sequestered from both contrast agents and may, therefore, be

(48) Altenbach, C.; Greenhalgh, D. A.; Khorana, H. G.; Hubbell, W. L. *Proc. Natl. Acad. Sci. U.S.A.* **1994**, *91*, 1667−1671.

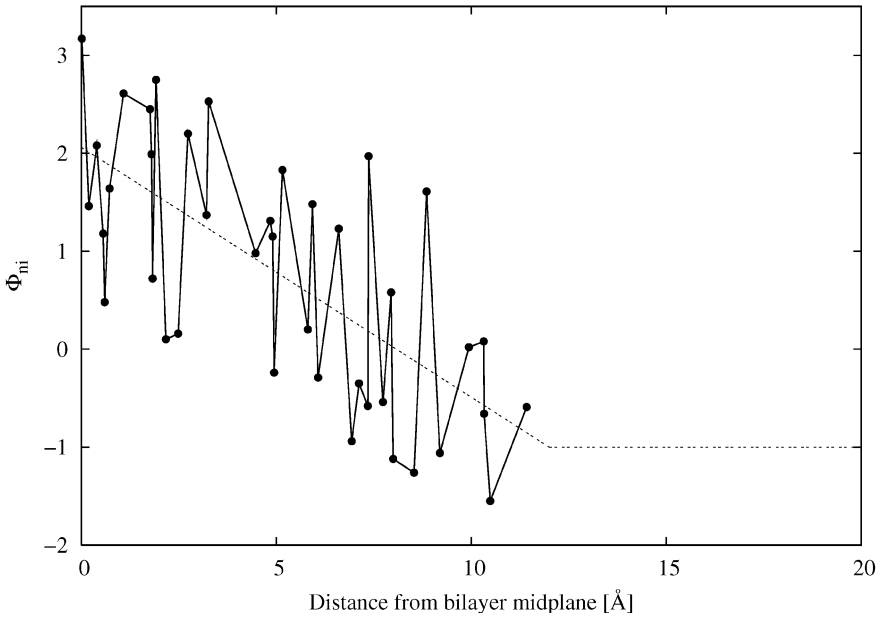

Figure 5. Experimentally determined depth parameter, $\Phi_i \equiv \ln\{[R_{1i}^{P}(O_2)/R_{1max}^{P}(O_2)]/[R_{wi}^{sat}/R_{wmax}^{sat}]\}$, as a function of the absolute value of immersion depth, z, using coordinates from the crystal structure and assuming a 25° tilt with respect to the micelle normal.[20] A linear interpolation over the region associated with the membrane interior (i.e., ±12 Å) reveals a Pearson r correlation of 0.69.

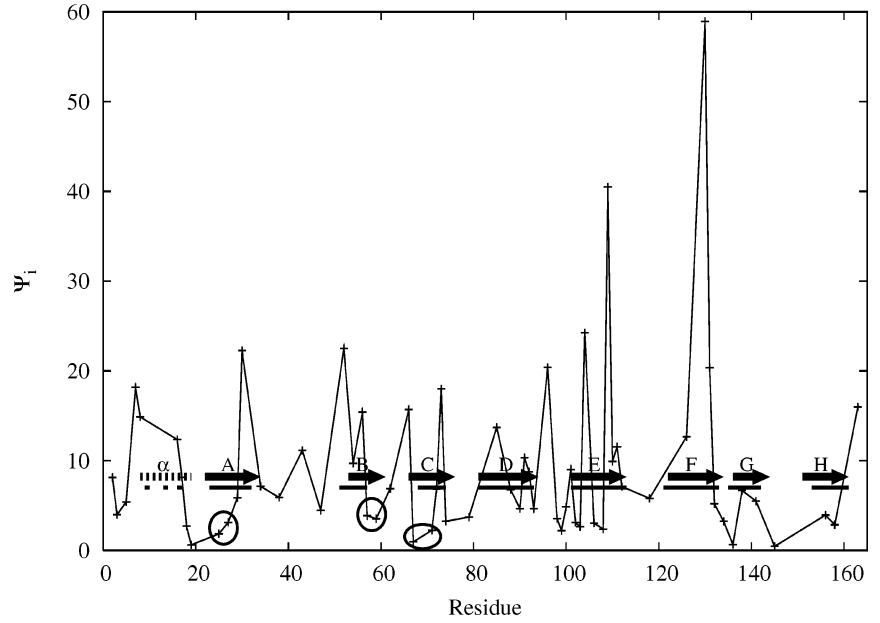

Figure 6. Steric profile, $\Psi_i \equiv R_{1i}^{P}(O_2)\, R_{wi}^{sat}$, as a function of residue, based on separate measurements of oxygen-induced paramagnetic relaxation rates, $R_{1i}^{P}(O_2)$, and water saturation. Key residues on the barrel surface, indicated by circles in the figure, exhibit low contrast effects from either water or oxygen, due to protection effects from the associated N-terminal α-helix. Conversely, very high values of Ψ_i are observed primarily on the extracellular side of the protein for transmembrane residues and are suggested to be associated with fast surface dynamics or exchange in regions of moderate hydrophobicity.

associated with the binding interface between the helix and the barrel. There are also other residues which exhibit low Ψ_i values between strands F and G, and these are likely due to other steric factors. It is also instructive to consider where Ψ_i is a maximum. Note that the global maximum which occurs in strand F at a serine residue presumably arises from rapid chemical exchange of water with the side-chain hydroxyl. Such residues are not reliable probes of bulk water and should be discounted. The remaining maxima occur in transmembrane residues near the membrane−water interface on the extracellular side. The existence of high contrast effects from water and oxygen is consistent with the notion of local disorder or cavitation effects,[49] possibly as a result of rapid surface dynamics.

Conclusions and Final Remarks

In this study, an analysis of contrast effects of oxygen from the measurement of paramagnetic relaxation rates associated with two-spin longitudinal order provided unique information on the residues associated with the transmembrane regions. In particular, high oxygen-induced paramagnetic rates were attributed to immersion depth, local protein hydrophobicity, and/

(49) Amovilli, C.; Floris, F. M. *Phys. Chem. Chem. Phys.* **2003**, *5*, 363−368.

or steric effects. The effect of local protein hydrophobicities on $R_{1i}^{P}(O_2)$ could be removed, to some extent, by considering an azimuthal average of $R_{1i}^{P}(O_2)$, leaving an immersion-depth-dependent paramagnetic rate profile. The shape of this depth-specific profile corroborated the hypothesis that the barrel axis does not lie along the immersion depth axis but is tilted by 25°, as proposed recently.[20] Complementary studies of water contact via the observation of amide decay rates during selective water saturation corroborated the assignment of transmembrane regions, while helping to identify residues associated with bulk and bound water. The combination of O_2 and water contrast studies by NMR provided details on the location of the binding interface between the N-terminal α-helix and the β-barrel. Furthermore, oxygen-induced rates and water contact information could be combined in a parameter Φ_i, which proved to correlate linearly with immersion depth.

Much of the information on PagP topology obtained from these experiments (i.e., tilt, hydrophobicity, and helix association) was not readily available from conventional solution NMR techniques, and it is anticipated that the approaches described will be useful for understanding structural and topological features of membrane proteins in general. The NMR O_2/H_2O scanning approach introduced in this paper presents a way in which additional information can be generated that is complementary to that derived from well-established NMR methodologies that involve measurement of NOE intensities or residual dipolar couplings. Moreover, although the focus in this paper involved the protein backbone, one can also expect at least the same sensitivity from similar measurements of side chains of membrane proteins and associated CH_3 protons.

Acknowledgment. This work was supported by grants from the Petroleum Research Council (R.S.P.), NSERC (R.S.P., L.E.K.), and the Canadian Institutes of Health Research (L.E.K.).

JA0610075